IOP Conference Series: Materials Science and Engineering

PAPER • **OPEN ACCESS**

Enhancement of Adhesion Force and Surface Conductivity of Graphene Oxide Films Using Different Solvents

To cite this article: F. M. El-Hossary *et al* 2020 *IOP Conf. Ser.: Mater. Sci. Eng.* **762** 012001

IOP Conf. Series: Materials Science and Engineering **762** (2020) 012001 doi:10.1088/1757-899X/762/1/012001

Enhancement of Adhesion Force and Surface Conductivity of Graphene Oxide Films Using Different Solvents

F. M. El-Hossary [1], Ahmed Ghitas [2], A. M. Abd El-Rahman [3, 1], A. A. Ebnalwaled [4], Mohammed. H. Fawey [1], M. Abdelhamid Shahat [2, *]

[1] Physics Department, Faculty of Science, Sohag University, Sohag, Egypt.
[2] National Research Institute of Astronomy and Geophysics (NRIAG), Solar and Space Research Department, Helwan, Cairo, Egypt.
[3] King AbdulAziz University, Jeddah, KSA.
[4] Electronics & Nano Devices Lab, Physics Department, Faculty of Science, South Valley University, Qena, 83523 Egypt

***** E-mail: m.abdelhamid999@gmail.com

Abstract. In this work, the nanotechnology procedure was utilized to improve both the adhesion force and surface properties of graphene oxide (GO) films. GO has been obtained in a powder form by oxidation purified graphite using the modified Hummer`s technique. Different films of GO nanoparticles (NPs) were deposited using several types of solvents distilled water, acetone, ethanol, dimethyl formamide (DMF) or ethylene glycol. Examination of structural and optical properties of GO films were studied by XRD and UV–vis absorption spectroscopy. Moreover, electrical properties, surface roughness, contact angle, adhesion force, wetting energy and spreading coefficient were investigated. It was observed that the properties of the prepared films are influenced by the solvent type. The electrical resistivity of films is highly dependent on the solvent type which exhibited the lowest value with distilled water. Furthermore, GO film synthesized with distilled water has the best values of adhesion force and average surface roughness (Ra) 143.4 mN/m and ~ 7.83 µm, respectively. These results are mostly attributed to hydrophilic cites and GO NPs agglomeration in the surface of films and the effects of their size leading to an expansion in the surface roughness.

Keywords: Graphene Oxide, GO Thin Films, Contact Angle, Adhesion Force, Surface Roughness, Electrical Resistivity.

1. Introduction

Numerous researchers have found a great deal of enthusiasm for metal oxide semiconductors materials due to their smart benefits in engineering applications, mainly in automobiles, integrated circuits, and biological industries. [1–3]. Graphene is a significant carbon form derived from graphite and as of late, it considered as an effective semiconductor material with zero energy gap [4–6]. It is synthesized in a monolayer or a few layers of a 2D planar sheet of sp^2 hybridized carbon atoms with hexagonal structure [7,8].

Graphene and its oxide derivatives have large surface area, great electrical conductivity, dependable mechanical properties, exceptional thermal stability and good optical properties [9]. Therefore, they connected to various applications, including high-energy storage, nanomachines, electronic circuits [10], medication [11] and high-performance photovoltaics [12-14].

Graphene oxide (GO) is directly synthesized by the oxidation of purified natural graphite using a changed Hummer's technique. As reported, hydroxyl, epoxide functional groups and carboxylic acid (eCOOH) species can

be obtained during the oxidation process of graphite; all groups are responsible for the dispersion stability in polar solvents [15]. The high concentration of oxygen-enriched functional groups expand the GO interlayer spacing and in turn increase its hydrophilic nature. Therefore, GO thin films can be used in the fabrication

process of polymer solar cells so as to enhance the chemical reactivity of the nanocomposite polymer layer [16-19].

As chemically known, identification of the appropriate solvent plays an important role in the synthesis process of GO films and accordingly improving their surface properties such as friction coefficient [20], optical properties [21], and thermal conductivity [22]. These surface characteristics, make it suitable material for many applications such as water desalination [23,24], gas separation [25,26], transparent conductive films [27], supercapacitors and fuel cells [28].

The mechanical and electrical characterization of industrial engineering materials can be simply explained by determining their surface wettability and surface energy [29–35]. Based on that, the wettability investigation has practical importance at the macroscopic-scale as well as at the nano-scale [36]. It leads to estimate the surface free energy, polar and dispersion energy beside the adhesion force of the film materials [37].

In this work, we concentrated on the synthesize of pure GO films with different solvent types such as distilled water, acetone, ethanol, DMF or ethylene glycol. This is to improve the electrical resistivity and surface adhesion of GO films by controlling the surface energy and attraction forces between the GO films and the glass substrate. Therefore, surface roughness, electrical conductivity, adhesion force, wetting energy and spreading coefficient were studied in order to evaluate the performance of GO films.

2. Experimental Setup

2.1. Materials

Sulfuric acid (H_2SO_4), phosphoric acid (H_3PO_4), graphite powder, potassium permanganate ($KMnO_4$, 99%) and hydrogen peroxide (H_2O_2; 30%) were used as precursors. Moreover, hydrochloric acid (HCL; 37%) and various types of a solvent such as distilled water, acetone, Ethanol, DMF and Ethylene Glycol were employed.

2.2. Synthesis of Graphene Oxide as powder form

GO in the powder form has been obtained by oxidation of the purified natural graphite using modified Hummer's technique as shown in Fig.1. In brief, three grams of graphite precursor were gradually added to 320ml of concentrated H_2SO_4 in a flask, which placed in magnetic stirrer. Then, 80ml of H_3PO_4 was added in a dropwise to the mixture under continuous stirring for 2h. After that, small portions of $KMnO_4$ (18g) were added slowly to the mixture in order to avoid fast temperature rising. The resultant combination was left for stirring for three days to allow the oxidation of graphite. The color solution changed from black to dark green. Thereafter, the H_2O_2 solution was added to terminate the oxidation process and remove the $KMnO_4$ at room temperature (RT). The resulting suspension was bright yellow in color, indicating a high level of oxidation graphite process [38, 39]. The formed graphene oxide was washed three times with (1M) of HCl aqueous solution to remove the remaining acid [40], and repeated with distilled water until a 6-7 pH was achieved. Finally, the obtained solution dried at 50˚C to obtain graphene oxide powder.

Figure 1. Preparation diagram of GO NPs

2.3. Synthesis Graphene Oxide (GO) Nanoparticles films

The clean process of the glass substrate is started using a dilute acidic solution of HCl followed by an extensive water rinse to remove the residual HCl. After that, it is sonicated in acetone from the surface of the conductive side, wet cleaned in ethanol and sonicate to remove organic impurities and finally rinse with deionized water. To deposit GO films, GO powder was added to different solutions such as distilled water, acetone, ethanol, DMF and ethylene glycol. The obtained suspensions were deposited by a spin coating on glass substrates using a 1000 rpm for 30 sec. Lastly, the obtained films were dried at 50°C.

3. Characterization

The phase purity and structure of the prepared films were characterized by X-ray diffraction (XRD) using Philips diffractometer with a Cu-target (λ=1.54056 Å) and a graphite monochromator. The optical properties of the GO films were studied using a computerized SPECORD 200 PLUS spectrophotometer with a 1 nm step, at normal incidence at RT in a wavelength range of 190-1100 nm. The contact angel analysis tool (SEO Phoenix 300) was used to measure contact angle, surface tension, wet energy, diffusion of power factor and adhesion force. Moreover, the surface roughness (Ra) was measured using the profilometer (Talysurf 50-Taylor Hopson precision). Furthermore, the four probes resistivity testing method was used to measure the resistivity by the EQ-JX2008-LD resistivity tester. All the measurements were carried out at RT (~ 26˚C).

4. Results and Discussion

4.1 Structure Analysis

The X-ray diffraction pattern of a prepared GO powder reveals a strong and sharp diffraction peak (001) demonstrating a preferred orientation of GO basal planes parallel to the sample plane as shown in Fig. 2. The oxidation degree of graphite and the interlayer spacing can be acquired. The reflection peak (002) of pure graphite happened at 2θ = 25~30˚ with an interlayer spacing around 0.34 nm [41]. After the oxidation process (forming GO), the reflected peak is gradually weakened and finally disappeared and then appears at 2θ = 10~15˚ with a d-spacing value of 0.6–1.0 nm [42, 43]**.** This peak shift demonstrates that graphite is totally converted to GO. The main factors controlling the estimation of the d spacing value of graphite are the degree of oxidation, the removal of oxygen atoms from the graphite gallery during intercalation, and the number of water molecules involved in the interlayer spacing [42, 44].

The d-spacing of GO can be calculated according to Bragg's law:

$$n\lambda = 2d\sin\theta \qquad (1)$$

where *n* is the diffraction series and λ is the wavelength of the X-ray beam, d is the distance between the adjacent GO sheets or layers and θ is the diffraction angle. Herein, after oxidizing process, the native sharp peak of the as prepared GO powder occurred at 2θ ~9.6˚ and the interlayer spacing increases to about 0.92 nm. This increase in interplanar distance owing to trap oxygen functional group between the sheets in graphite structure [45]. graphite exfoliation has occurred in individual graphene oxide sheets (single or multi-layer) [46].

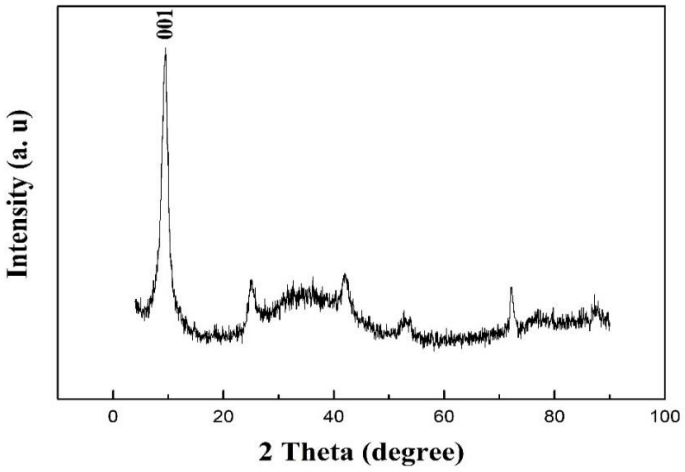

Figure 2. XRD spectra of GO film

4.2 Optical Properties

An UV-visible spectrophotometer was employed to measure the absorbance spectra of GO films, over a spectral range from 300 nm to 800 nm, which deposited using different solvents and are shown in Fig. 3. During graphite oxidation, oxygen binds to the graphene layers, which improves the layers polarity and thus improves their solubility in water [47]. These result leads to a change in the solution color from yellow to brown. It was noted that the edge of GO films uptake is about 320 nm without any change when using different solvents. On the other hand, the optical energy gap of the prepared films was determined using the universal method Tauc relationship for direct transition semiconductor materials [48].

$$\alpha h\nu = B\left(h\nu - E_g\right)^r \qquad (2)$$

Where hν is photon energy and B is a parameter which is related to the transition probability, α is the absorption coefficient, Eg is the optical band gap and r is a number that distinguishes the transition process; having a value of 1/2 for direct allowed [49]. The optical band gap values Eg were calculated and are shown in Fig. 4. Based on that, a high change is obtained for the Eg values of GO films, indicating values of 3.52, 3.56, 3.59, 3.62 and 3.67 eV for the samples deposited with several types of solvent distilled water, acetone, ethanol, DMF and ethylene glycol, respectively. Improvement of the value of the energy band gap to 3.52 eV with distilled water solvent offers high potential GO films for electronic applications.

These results may be related to the various arrangements of agglomeration epoxide functional groups and carboxylic inside GO films and the high surface roughness value in GO film which synthesized with distilled water. The change in surface roughness of the GO films affects their optical properties including transmittance, absorbance and optical constants [50, 51].

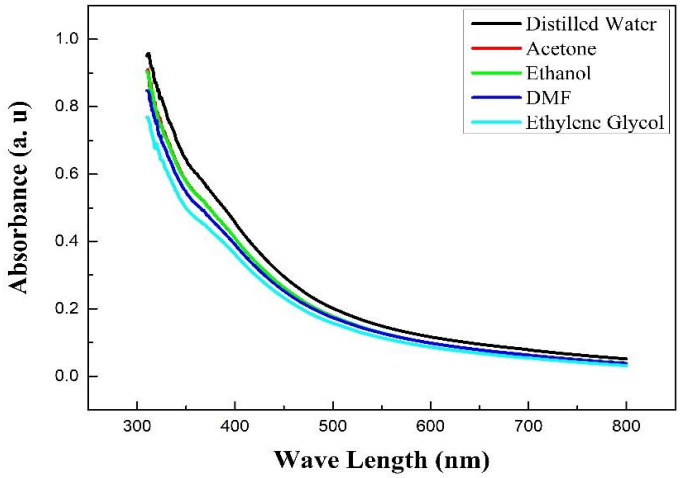

Figure 3. UV-VIS absorption spectra for GO films with different solvent types

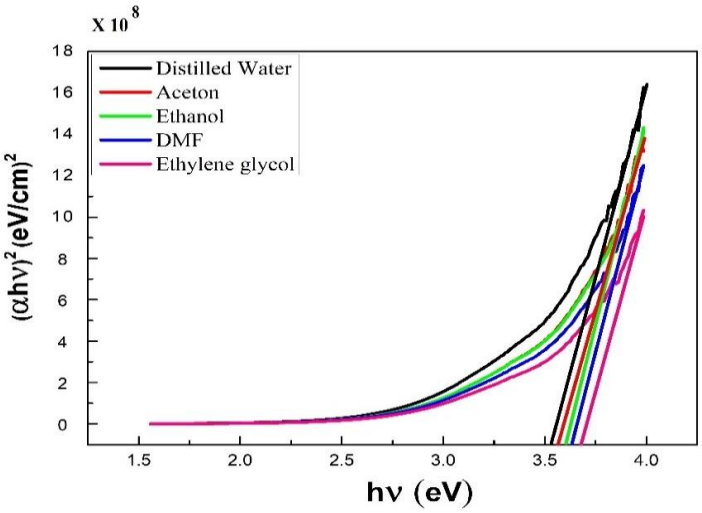

Figure 4. The relation between $(\alpha h\nu)^2$ and hν for GO films with different solvent types

4.3 Contact Angle

Contact angle (average in degree) and surface tension measurements of pure GO films, which dissolved in various solvents such as distilled water, acetone, ethanol, DMF and ethylene glycol were investigated. Contact angle value is highly depending on the utilized solvent type, which shows verities value from 14.11° to 30° for distilled water and ethylene glycol solvents as one can see from Fig. 5. additionally, the adhesion force between deposited GO films and water by calculating the work of adhesion with the equation [52]:

$$Wsl = \gamma s + \gamma l + \gamma sl \quad (3)$$

where γs, γ*l*, and γs*l* are the solid surface free energy, liquid (water, in this study) surface free energy, and solid–liquid interfacial energy, respectively. Combining with Young-Dupré equation

$$\gamma s = \gamma sl + \gamma l \cos \theta_e \quad (4)$$

gives the equation [53]:

$$Wsl = \gamma l \, (1 + \cos \theta_e) \quad (5)$$

where θ_e is the equilibrium (Young's) contact angle between oxidized GO films and water, γ_L is the surface tension of water on the solid surface.

Fig .6 demonstrates that the contact angle and adhesion force of GO films are influenced by the dissolvable type. When the contact angle value was gradually increasing, the adhesion work decreased. Utilizing different solvents for synthesizing GO films leading to changes in the surface properties from hydrophobic to hydrophilic films. Using distilled water solvent for depositing GO film demonstrated to increase the hydrophilicity and has the best value of adhesion force reveals to 143.4 (mN/m).

Fig. 6 a,b represents the dependence of the spreading coefficient and wetting energy of GO films on the solvent type. The solvent type has a high effect on surface properties, leading to an improvement in the wettability of water on the GO surface. Utilizing various types of solvent for deposition GO films leads to rearrange many hydrophilic spices that in order enhance the wettability of GO films [54–57]. The arrangement of more hydrogen bonds between the used water and GO films cause an increase in the dipole/dipole interaction, which in turn improves the wettability [58, 59]. Fig. 7a demonstrates emotional improvement in the wettability that happened by utilizing distilled water as the solvent reveals to 70.6 (mN/m). In addition, the solvent type can be chosen to improve spreading coefficient GO thin films to -2.19 (mN/m) for distilled water as shown in Fig. 7b. The fundamental explanations for these outcomes are the surface roughness [60,61] and the molecular interactions [62].

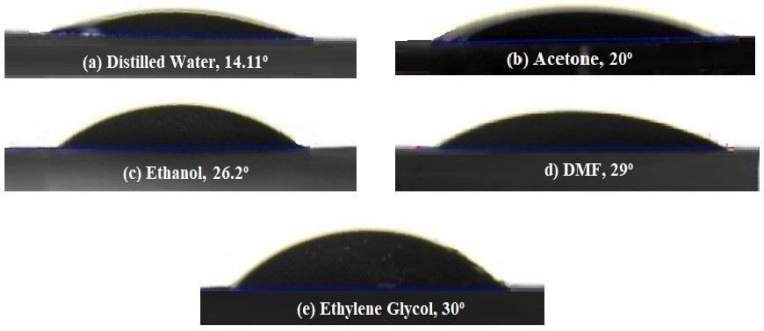

Figure 5. Contact angles and interfaces between water droplets and GO films.

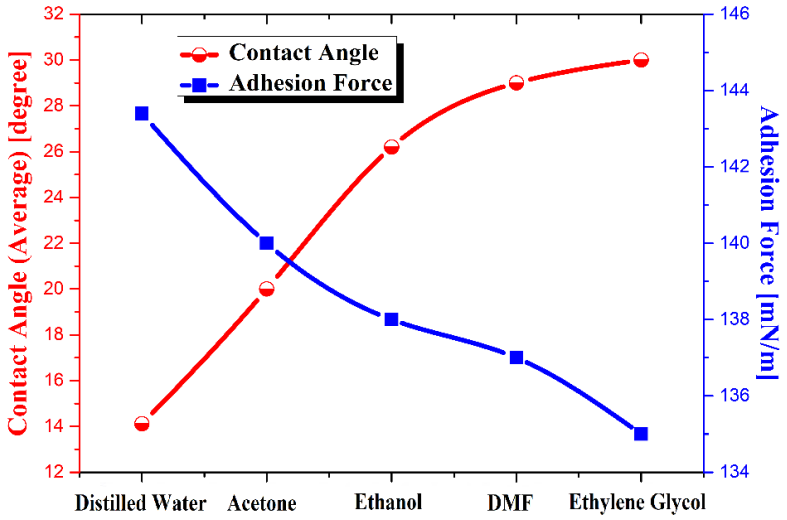

Figure 6. Effect of solvent type on the contact angle and adhesion force for GO films

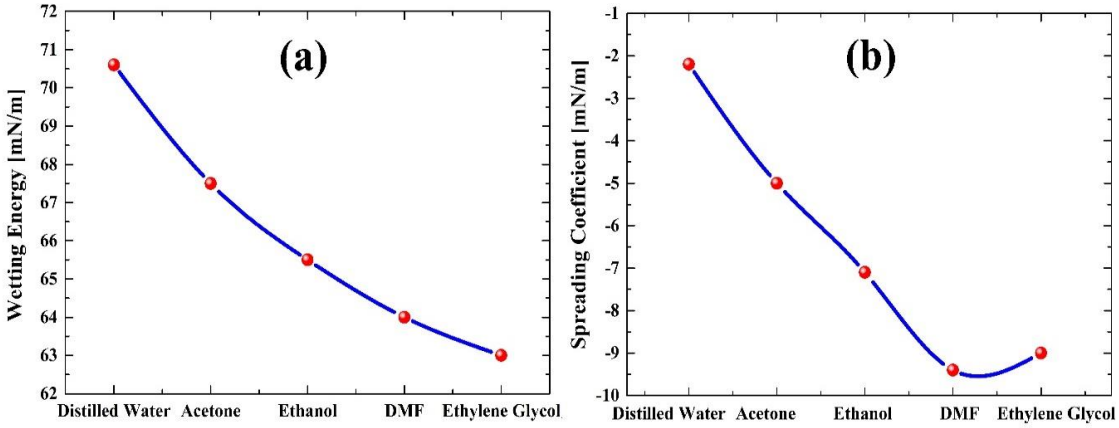

Figure 7. (a)The dependence of wetting energy, (b) spreading coefficient of GO films on solvent type

4.4 Surface Roughness Measurement

The roughness behavior is considerably different when GO films synthesized in various solvents. Fig 8. shows a relatively flat surface reduces the value of the surface roughness. The average roughness value (Ra) decreased from ~7.83 μm for distilled water solvent to ~3.75 μm for ethylene glycol. These outcomes are generally attributed to the agglomeration of GO nanoparticles in films surface and their size impacts lead to an expansion in surface roughness. However, the fibrous network structure is generally responsible for the surface smoothness. The obtained results are showing good agreement with the contact angle performances.

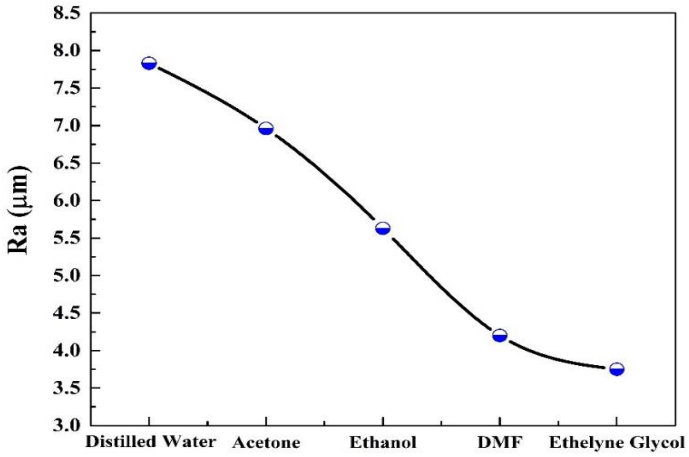

Figure 8. The average surface roughness behavior of GO films using different solvent types

4.5 Electrical Properties of GO Films

Of the generally recognized Lerf-Klinowski model for the GO structure, the basal plane of GO films contains functional groups of hydroxyl and epoxide, though the edges of GO are mainly oxidized with quinoidal and carboxylic acid species [63]. These oxygen-containing moieties give advantageous chemical handles to the expansion of other functional groups to graphene, for example alkyl gatherings, amines, and polymer chains.

Along these lines, we have been synthesized GO films using several solvent types to improve the charge carrier's mobility and reduce the electrical resistivity. The resistivity measured by 4PP method approved that; the electrical resistivity and conductivity of the obtained films are highly dependent on the types of solvents used. For the GO bulk material, the sheet resistivity determined from Van der Pauw measurements to be 1.62 MΩ/square, yielding a value of −3.1 S/m for the bulk conductivity [64]. In the present investigation, taking into account the GO film thickness of about 100 microns, the sheet resistivity values are 0.095, 0.16, 0.1, 0.12 and 0.25 MΩ/square for the samples synthesized with solvents distilled water, acetone, ethanol, DMF and ethylene glycol, respectively as shown in Fig. 9. These obtained outcomes confirmed that distilled water solvent enhances the GO film performance and displayed an optimum value of electrical conductivity (0.11 S/m), meanwhile the existence of oxygenated groups deteriorates the electrical conduction of GO. In our case, the various electrical insulation value of synthesized GO films peppered in different solvents can be attributed mainly to the presence of a homogeneouse electrical dispersion causing various arrangements of agglomeration epoxide functional groups and carboxylic inside the GO films, and at the same time the existence of oxygenated groups [65, 66]. These result in the immobilization and obstruction of charge carriers and deteriorates the electrical conduction of GO [67,68]. Having a highly conductive GO film is synthesized in distilled water can enhance electron transfer in the framework, thus improving their electrical conductivity.

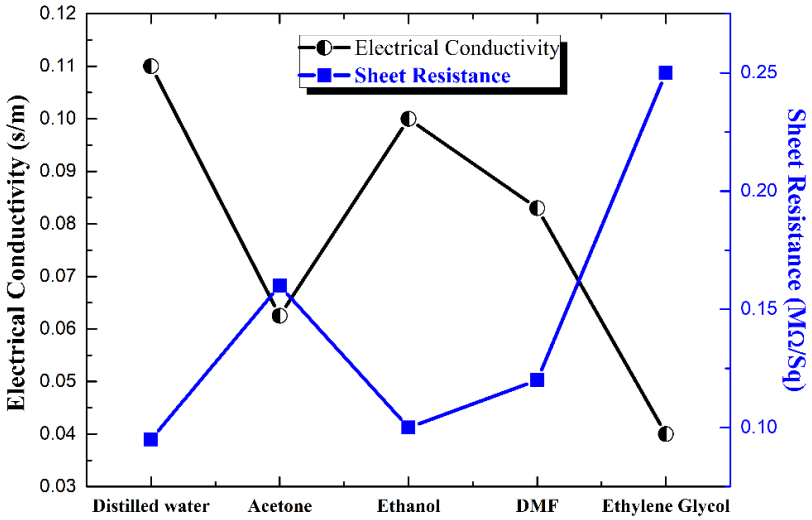

Figure 9. Electrical conductivity and sheet resistance behavior of GO films synthesized with different solvent

5. Concluding remarks

In his work, it can conclude the following points:

- Successfully synthesize metal oxide material GO NPs by oxidation purified natural graphite using modified Hummer's technique.
- GO film synthesized in distilled water solution exhibited the lowest value of electrical resistivity, and has the optimum value of adhesion force (143.4 mN/m) and average surface roughness (Ra) of ~7.83 µm.
- The obtained results are generally attributed to hydrophilic cites and the agglomeration of GO NPs in the film's surface and their size effect leads to an expansion in the surface roughness.
- The high conductivity value obtained from the GO film (0.11 S/m), which is synthesized in distilled water, can enhance the electron transfer in the framework, owing to the good arrangement of agglomeration epoxide functional groups and carboxylic inside GO film leading to improve their electrical conductivity.

References

[1] Shen, S., & Meng, Y. (2012). *Tribology Letters*, *47*(2), 273-284.
[2] Tambe, N. S., & Bhushan, B. (2004). *Nanotechnology*, *15*(11), 1561.
[3] Alfeeli, B., Cho, D., Ashraf-Khorassani, M., Taylor, L. T., & Agah, M. (2008). *Sensors and Actuators B: Chemical*, *133*(1), 24-32.
[4] J. Wei, J., Zang, Z., Zhang, Y., Wang, M., Du, J., & Tang, X. (2017). *Optics letters*, *42*(5), 911-914.
[5] Huang, H., Zhang, J., Jiang, L., & Zang, Z. (2017). *Journal of Alloys and Compounds*, *718*, 112-115.
[6] Zang, Z., Zeng, X., Wang, M., Hu, W., Liu, C., & Tang, X. (2017). *Sensors and Actuators B: Chemical*, *252*, 1179-1186.
[7] Anand, K., Singh, O., Singh, M. P., Kaur, J., & Singh, R. C. (2014). *Sensors and Actuators B: Chemical*, *195*, 409-415.
[8] Subramani, K., & Sathish, M. (2019). *Materials Letters*, *236*, 424-427.
[9] Park, J. W., Lee, C., & Jang, J. (2015). *Sensors and Actuators B: Chemical*, *208*, 532-537.
[10] Asadi, K., Timmering, E. C., Geuns, T. C., Pesquera, A., Centeno, A., Zurutuza, A., ... & de Leeuw, D. M. (2015). *ACS applied materials & interfaces*, *7*(18), 9429-9435.
[11] Shen, H., Zhang, L., Liu, M., & Zhang, Z. (2012). *Theranostics*, *2*(3), 283.
[12] Acik, M., & Darling, S. B. (2016). *Journal of Materials Chemistry A*, *4*(17), 6185-6235.
[13] Rafiee, M. A., Rafiee, J., Wang, Z., Song, H., Yu, Z. Z., & Koratkar, N. (2009). *ACS nano*, *3*(12), 3884-3890.
[14] Park, S., & Ruoff, R. S. (2009). *Nature nanotechnology*, *4*(4), 217.
[15] Sarno, M., Senatore, A., Cirillo, C., Petrone, V., & Ciambelli, P. (2014). *Journal of nanoscience and nanotechnology*, *14*(7), 4960-4968.
[16] Dreyer, D. R., Park, S., Bielawski, C. W., & Ruoff, R. S. (2010). *Chemical society reviews*, *39*(1), 228-240.
[17] Dreyer, D. R., Todd, A. D., & Bielawski, C. W. (2014). *Chemical Society Reviews*, *43*(15), 5288-5301.
[18] Tang, Q., Zhou, Z., & Chen, Z. (2013). *Nanoscale*, *5*(11), 4541-4583.
[19] Lerf, A., He, H., Forster, M., & Klinowski, J. (1998). *The Journal of Physical Chemistry B*, *102*(23), 4477-4482.
[20] Berman, D., Erdemir, A., & Sumant, A. V. (2014). *Materials Today*, *17*(1), 31-42.
[21] Kim, K. K., Reina, A., Shi, Y., Park, H., Li, L. J., Lee, Y. H., & Kong, J. (2010). *Nanotechnology*, *21*(28), 285205.
[22] Zhang, C., Hao, X. L., Wang, C. X., Wei, N., & Rabczuk, T. (2017). *Scientific reports*, *7*, 41398.
[23] Abraham, J., Vasu, K. S., Williams, C. D., Gopinadhan, K., Su, Y., Cherian, C. T., ... & Carbone, P. (2017). *Nature nanotechnology*, *12*(6), 546.
[24] Chen, L., Li, Y., Chen, L., Li, N., Dong, C., Chen, Q., ... & Zhang, L. (2018). *Chemical Engineering Journal*, *345*, 536-544.
[25] Chi, C., Wang, X., Peng, Y., Qian, Y., Hu, Z., Dong, J., & Zhao, D. (2016). *Chemistry of Materials*, *28*(9), 2921-2927.
[26] Yoo, B. M., Shin, J. E., Lee, H. D., & Park, H. B. (2017). *Current opinion in chemical engineering*, *16*, 39-47.
[27] Zheng, Q., Li, Z., Yang, J., & Kim, J. K. (2014). *Progress in Materials Science*, *64*, 200-247.
[28] Gao, W., Wu, G., Janicke, M. T., Cullen, D. A., Mukundan, R., Baldwin, J. K., ... & Dattelbaum, A. M. (2014). *Angewandte Chemie International Edition*, *53*(14), 3588-3593.
[29] Barranco, A., Borras, A., Gonzalez-Elipe, A. R., & Palmero, A. (2016). *Progress in Materials Science*, *76*, 59-153.
[30] Nieuwenhuizen, J. M., & Haanstra, H. (1966). *Philips Tech Rev*, *27*(3), 87-91.
[31] Lewis, B., & Campbell, D. S. (1967). *Journal of vacuum science and technology*, *4*(5), 209-218.
[32] Nakhodkin, N. G., & Shaldervan, A. I. (1972). *Thin Solid Films*, *10*(1), 109-122.
[33] Dirks, A. G., & Leamy, H. J. (1977). *Thin Solid Films*, *47*(3), 219-233.

[34] van Kranenburg, H., & Lodder, C. (1994). *Materials Science and Engineering: R: Reports*, *11*(7), 295-354.
[35] Kwan, J. K., & Sit, J. C. (2013). *Sensors and Actuators B: Chemical*, *181*, 715-719.
[36] Nakamura, Y., Carlson, A., Amberg, G., & Shiomi, J. (2013). *Physical Review E*, *88*(3), 033010.
[37] Torrisi, V., & Ruffino, F. (2017). *Surface and Coatings Technology*, *315*, 123-129.
[38] Kovtyukhova, N. I., Ollivier, P. J., Martin, B. R., Mallouk, T. E., Chizhik, S. A., Buzaneva, E. V., & Gorchinskiy, A. D. (1999). *Chemistry of materials*, *11*(3), 771-778.
[39] He, G., Chen, H., Zhu, J., Bei, F., Sun, X., & Wang, X. (2011). *Journal of Materials Chemistry*, *21*(38), 14631-14638.
[40] William, S., Hummers, J. R., & Offeman, R. E. (1958). *J. Am. Chem. Soc*, *80*(6), 1339-1339.
[41] Saleem, H., & Habib, A. (2016). *Journal of Alloys and Compounds*, *679*, 177-183.
[42] Ramesh, P., Bhagyalakshmi, S., & Sampath, S. (2004). *Journal of colloid and interface science*, *274*(1), 95-102.
[43] McAllister, M. J., Li, J. L., Adamson, D. H., Schniepp, H. C., Abdala, A. A., Liu, J., ... & Aksay, I. A. (2007). *Chemistry of materials*, *19*(18), 4396-4404.
[44] Van Blaaderen, A., & Kentgens, A. P. M. (1992). *Journal of Non-Crystalline Solids*, *149*(3), 161-178.
[45] Lerf, A., He, H., Forster, M., & Klinowski, J. (1998). *The Journal of Physical Chemistry B*, *102*(23), 4477-4482.
[46] Wang, H., & Hu, Y. H. (2011). *Industrial & Engineering Chemistry Research*, *50*(10), 6132-6137.
[47] Leffler, J. (2012). *Luleå University*.
[48] Pankove, J. I. (1975). *Optical processes in semiconductors*. Courier Corporation.
[49] Ahmadi, M., Ghasemi, M. R., & Rafsanjani, H. H. (2011. Journal of Materials Science and Engineering, 5, 87-93.
[50] Fang, J., Wang, J., Cao, X., Man, Y., Liu, C., Cheng, L., ... & Li, J. (2018). *Journal of Physics Communications*, *2*(1), 015009.
[51] Sreeja, S., Frobel, P. L., Mayadevi, S., Suresh, S. R., & Muneera, C. I. (2015). In *IOP Conference Series: Materials Science and Engineering* (Vol. 73, No. 1, p. 012116). IOP Publishing.
[52] Leroy, F., & Müller-Plathe, F. (2010). *The Journal of chemical physics*, *133*(4), 044110.
[53] Psarski, M., Pawlak, D., Grobelny, J., & Celichowski, G. (2019). *Applied Surface Science*, *479*, 489-498.
[54] Bronco, S., Bertoldo, M., Taburoni, E., Cepek, C., & Sancrotti, M. (2004, November). In *Macromolecular Symposia* (Vol. 218, No. 1, pp. 71-80). Weinheim: WILEY-VCH Verlag.
[55] Arpagaus, C., Rossi, A., & Von Rohr, P. R. (2005). *Applied Surface Science*, *252*(5), 1581-1595.
[56] Novák, I., & Florián, Š. (2004). *Journal of materials science*, *39*(6), 2033-2036.
[57] Novák, I., Pollak, V., & Chodak, I. (2006). *Plasma Processes and Polymers*, *3*(4-5), 355-364.
[58] Yang, L., Chen, J., Guo, Y., & Zhang, Z. (2009). *Applied Surface Science*, *255*(8), 4446-4451.
[59] Owens, D. K., & Wendt, R. C. (1969). *Journal of applied polymer science*, *13*(8), 1741-1747.
[60] Siddiqa, A. J., Chaudhury, K., & Adhikari, B. (2015). *Res. Rev. J. Med. Chem*, *1*, 43-54.
[61] Sanchis, R. M., Calvo, O., Sánchez, L., García, D., & Balart, R. (2007). *Journal of Polymer Science Part B: Polymer Physics*, *45*(17), 2390-2399.
[62] Carré, A. (2007). *Journal of Adhesion Science and Technology*, *21*(10), 961-981.
[63] Lerf, A., He, H., Forster, M., & Klinowski, J. (1998). *The Journal of Physical Chemistry B*, *102*(23), 4477-4482.
[64] Banerjee, I., Mahapatra, S. K., Pal, C., Sharma, A. K., & Ray, A. K. (2018). *Materials Research Express*, *5*(5), 056405.
[65] Liang, K., Shi, L., Zhang, J., Cheng, J., & Wang, X. (2018). *Thermochimica acta*, *664*, 1-15.
[66] Owais, M., Zhao, J., Imani, A., Wang, G., Zhang, H., & Zhang, Z. (2019). *Composites Part A: Applied Science and Manufacturing*, *117*, 11-22.
[67] Gao, Y., Gu, A., Jiao, Y., Yang, Y., Liang, G., Hu, J. T., ... & Yuan, L. (2012). *Polymers for Advanced Technologies*, *23*(5), 919-928.

[68] Huang, X., Zhi, C., Jiang, P., Golberg, D., Bando, Y., & Tanaka, T. (2013). *Advanced Functional Materials*, *23*(14), 1824-1831.